
	ITTC – Recommended Procedures and Guidelines	7.5-02 06-04 Page 1 of 25	
	Forces and moment Uncertainty Analysis, Example for Planar Motion Mechanism Test	Effective Date 2008	Revision 00

Table of Contents

Uncertainty Analysis, Example for Planar Motion Mechanism Test 2	2.4.2 Precision Limit 12 2.4.3 UA Results 13
1. PURPOSE OF PROCEDURE 2	3. REFERENCES 15
2. EXAMPLE FOR PMM TEST 2	Appendix A Mean draft bias B_{Tm} 21
2.1 Test Design 3	Appendix B.. Moment of inertia bias B_{Iz}.... 21
2.2 Data Acquisition and Reduction 4	Appendix C Carriage speed bias B_{Uc}..... 24
2.3 Measurement Systems and Procedures 5	Appendix D Drift angle bias B_{β}..... 24
2.4 Uncertainty Analysis 7	
2.4.1 Bias Limit 7	

Edited	Approved
Manoeuvring Committee of 25 th ITTC	25 th ITTC 2008
Date 2008	Date 09/2008

	ITTC – Recommended Procedures and Guidelines	7.5-02 06-04 Page 2 of 25	
	Forces and moment Uncertainty Analysis, Example for Planar Motion Mechanism Test	Effective Date 2008	Revision 00

Uncertainty Analysis, Example for Planar Motion Mechanism Test

1. PURPOSE OF PROCEDURE

The purpose of the procedure is to provide an example for the uncertainty analysis (UA) of a model scale towing tank planar motion mechanism (PMM) test following the ITTC Procedures 7.5-02-01-01 Rev 00, ‘Uncertainty Analysis in EFD, Uncertainty Assessment Methodology’ and 7.5-02-01-02 Rev 00, ‘Uncertainty Analysis in EFD, Guidelines for Towing Tank Tests.’ Present UA procedure is developed in collaboration between IIHR-Hydro science & Engineering (IIHR), Force Technology, Instituto Nazionale per Studi ed Esperienze di Architettura Navale (INSEAN), and the 24th – 25th ITTC Manoeuvring Committee, including overlapping tests using the same model geometry for comparison of results and identification of facility biases and scale effects. Details of the UA procedures are provided by Simonsen (2004), Benedetti et al. (2006), and Yoon et al. (2007), including in the latter case comparisons between facilities and analysis of facility biases, scale effects, and parameter trends. Section 10 of the 25th ITTC Manoeuvring Committee Report summarizes the overlapping tests and results. The following example is based on the IIHR results.

2. EXAMPLE FOR PMM TEST

This procedure provides an example of uncertainty assessment for a model scale towing tank PMM test for an un-appended model ship except bilge keels (i.e. without shafts, struts, propellers, and rudders) which is mounted free to heave and pitch, but fixed in roll. The PMM test conforms to the ITTC Procedures 7.5-02-

06-02 Rev02, ‘Captive Model Test Procedure.’ Bias and precision limits and total uncertainties for multiple runs are estimated for the non-dimensional forces and moment in model scale for four types of PMM tests (static drift, pure yaw, pure sway, and yaw and drift) at one Froude number ($Fr = 0.280$). Other PMM tests, such as static rudder, static drift and rudder, static drift and heel, dynamic yaw and rudder, dynamic yaw and drift and rudder, are not considered. This procedure does not provide UA for hydrodynamic derivatives derived from the forces and moment data or their effect on the full scale manoeuvring simulations. Additionally, UA estimates for heave and pitch are not provided.

The effect of data conditioning such as filtering or fairing, for example, Fourier Series (FS) reconstructions for the measured forces/moment and motions is not counted in this UA procedure. This procedure assumes that the measured forces/moment is the sum of those from all forces/moment gauges used for the case of multiple gauge system, and that the inertia forces/moment from parts for model installation are subtracted from the total measured forces and moments if the parts are suspended from the load cells. This procedure also assumes that the model ship is free to heave and pitch, and fixed in roll. The effect of deviations from the upright position such as roll or heel angle is not considered in this procedure. Finally, carriage speed is assumed to be constant, so the effect of acceleration caused by fluctuating carriage speed during runs is not considered.

2.1 Test Design

The tests are conducted in the IHR towing tank, which is 100m long, 3.048m wide and 3.048m deep, and equipped with a drive carriage, PMM carriage, automated wave dampener system, and wave-dampening beach. A right-handed Cartesian coordinate system is fixed to the model. The origin is at the intersection of the mid-ship plane, centreplane, and waterplane. The x , y , z axes are directed upstream, transversely to starboard, and downward, respectively (See Figure 1).

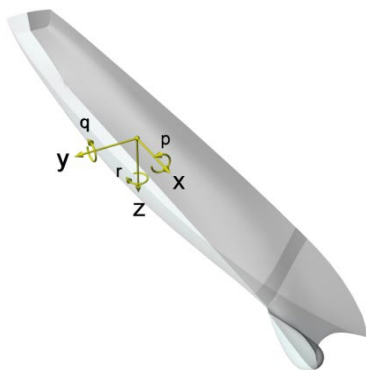


Figure 1 Coordinate system.

The model geometry is DTMB model 5512, a 1:46.6 scale, $L_{PP} = 3.048$ m. The model is unappended except for port and starboard bilge keels, i.e., not equipped with shafts, struts, propellers, or rudders. To initiate transition to turbulent flow, a row of cylindrical studs of 1.6 mm height and 3.2 mm diameter are fixed with 9.5 mm spacing at $x/L_{PP} = 0.45$. The stud dimensions and placement on the model are in accordance with the recommendations by the 23rd ITTC (ITTC, 2002). Model- and full-scale geometric parameters for 5512 are summarized in Table 1.

		Ship	Model
λ	-	1 : 1	1 : 46.588
L_{PP}	m	142.00	3.048
L_{WL}	m	142.18	3.052
B_{WL}	m	19.10	0.410
T_m	m	6.16	0.136
∇	m ³	8472	0.084
Δ	Ton	8684	0.086
C_B	-	0.506	0.506
A_{WP}	m ²		0.979
m	Kg		82.55
x_G	m		-0.0157
y_G	m		0.0000
I_z	Kg·m ²		49.99

Table 1 Full and model scale particulars.

See detail A

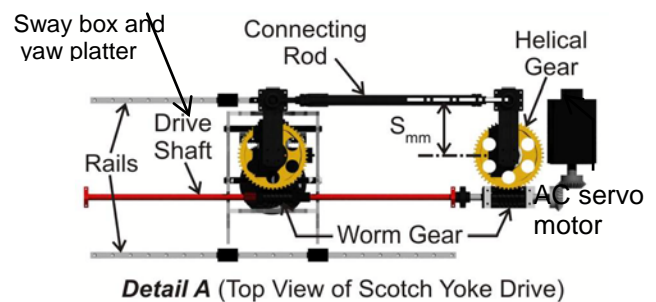
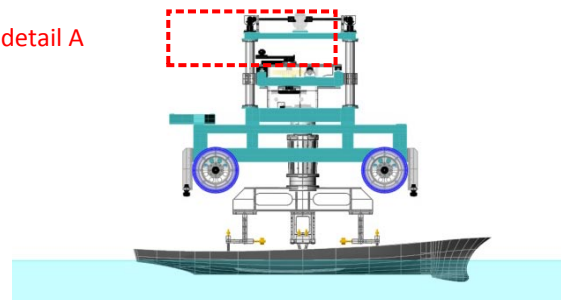



Figure 2 Side view of the PMM carriage and model ship mount (top), and close up of the scotch yoke drive (bottom).

 INTERNATIONAL TOWING TANK CONFERENCE	ITTC – Recommended Procedures and Guidelines	7.5-02 06-04 Page 4 of 25	
	Forces and moment Uncertainty Analysis, Example for Planar Motion Mechanism Test	Effective Date 2008	Revision 00

The model is ballasted with respect to port and starboard draft markers, and then connected to a mount with three ball-bearing type contacts which allows the model to move freely in pitch and heave, but constrains roll motion (See Figure 2). The mount is suspended from the load cell which is fixed at the PMM carriage. The mass and yaw moment of inertia of the mount are measured to correct their effects on the measured forces and moment at the data reductions phase of the test.

Fr	U_C	β	v'^{\dagger}
[-]	[m/s]	[deg.]	[-]
0.280	1.531	-10	-0.174

$$\dagger v' = \frac{v}{U_C}$$

Table 2 Test conditions for static drift test.

Fr	U_C	β_{corr}^*	N	S_{mm}	$v'_{\text{max}}{}^{\dagger}$	$\dot{v}'_{\text{max}}{}^{\ddagger}$
[-]	[m/s]	[deg]	[rpm]	[m]	[-]	[-]
0.280	1.531	10	8.0210	0.1584	0.174	0.291

$$*\beta_{\text{corr}} = \frac{v_{\text{max}}}{U}, \dagger v'_{\text{max}} = \frac{v_{\text{max}}}{U}, \ddagger \dot{v}'_{\text{max}} = \frac{\dot{v}_{\text{max}} L_{\text{PP}}}{U}$$

Table 3 Test conditions for pure sway test.

Fr	U_C	N	S_{mm}	ψ_0	$r'_{\text{max}}{}^{\dagger}$	$\dot{r}'_{\text{max}}{}^{\ddagger}$
[-]	[m/s]	[rpm]	[m]	[deg.]	[-]	[-]
0.280	1.531	8.0210	0.1636	10.2	0.30	0.50

$$\dagger r'_{\text{max}} = \frac{r_{\text{max}} L_{\text{PP}}}{U}, \ddagger \dot{r}'_{\text{max}} = \frac{\dot{r}_{\text{max}} L_{\text{PP}}^2}{U^2}$$

Table 4 Test conditions for pure yaw test.

Fr	U_C	β	N	S_{mm}	ψ_0	r'_{max}	\dot{r}'_{max}
[-]	[m/s]	[deg]	[rpm]	[m]	[deg]	[-]	[-]
0.280	1.531	10	8.0210	0.1636	10.2	0.30	0.50

Table 5 Test conditions for yaw and drift test.

Static drift test is conducted at the drift angle $\beta = -10^\circ$; pure sway test at the corresponding drift angle $\beta_{\text{corr}} = 10^\circ$; pure yaw test at $r'_{\text{max}} = 0.3$; and yaw and drift test at the same yaw rate of the pure yaw test with a drift angle $\beta = 10^\circ$. The details of each test condition are presented in Tables 2 – 5. Test conditions in the present procedure are a part of the full test matrix in Yoon et al. (2007), which conforms to the ITTC Procedures 7.5-02-06-02 Rev02, ‘Captive Model Test Procedure.’


2.2 Data Acquisition and Reduction

The present interest is in data acquisition of carriage speed U_C , ship model motions (y, ψ), and forces and moments (F_x, F_y, M_z) for static and dynamic PMM tests. All variables are acquired as time histories through each carriage run. Static test variables (F_x, F_y, M_z) are time-averaged whereas dynamic test variables (y, ψ, F_x, F_y, M_z) are treated with harmonic analysis in the data reduction phases of the study. The measurement details for U_C are presented in Longo and Stern, (2005).

If it is assumed that the vessel moves in the horizontal plane only (surge, sway, and yaw), the motion equations are reduced to the following equations:

$$\begin{aligned}
-F_x + X &= m(\dot{u} - vr - x_G r^2 - y_G \dot{r}) \\
-F_y + Y &= m(\dot{v} + ur - y_G r^2 + x_G \dot{r}) \\
-M_z + N &= I_z \dot{r} + m(x_G(\dot{v} + ur) - y_G(\dot{u} - rv))
\end{aligned} \tag{1}$$

where, X, Y, N are the hydrodynamic forces and moment, m is the mass of the model ship, I_z is the yaw moment of inertia of the model ship, x_G is the longitudinal distance from mid-ship to model ship centre of gravity (COG), y_G is the transverse distance from centerplane to

 INTERNATIONAL TOWING TANK CONFERENCE	ITTC – Recommended Procedures and Guidelines	7.5-02 06-04 Page 5 of 25	
	Forces and moment Uncertainty Analysis, Example for Planar Motion Mechanism Test	Effective Date 2008	Revision 00

model ship COG, u , v , r are surge, sway, yaw velocities, respectively, \dot{u} , \dot{v} , \dot{r} are surge, sway, yaw accelerations, respectively. In general $y_G=0$ for conventional marine vessels, but it is assumed to be non-zero for the purpose of uncertainty assessment. Equations (1) can be non-dimensionalized using water density ρ , advance speed $U = \sqrt{u^2 + v^2}$, mean draft T_m , and ship model length L_{PP} . The non-dimensional variables are denoted with a prime symbol and represent the data reduction equations (DRE's) for the measurements herein.

$$X' = \frac{F_x + m(\dot{u} - vr - x_G r^2 - y_G \dot{r})}{1/2 \rho U^2 T_m L_{PP}} \quad (2)$$

$$Y' = \frac{F_y + m(\dot{v} + ur - y_G r^2 + x_G \dot{r})}{1/2 \rho U^2 T_m L_{PP}} \quad (3)$$

$$N' = \frac{M_z + I_z \dot{r} + m(x_G(\dot{v} + ur) - y_G(\dot{u} - rv))}{1/2 \rho U^2 T_m L_{PP}^2} \quad (4)$$

Although equations (2-4) are technically applicable DRE's for all tests herein, they can be simplified considerably by dropping the inertia terms for the case of the static drift tests which is done below in equations (5-7).

$$X' = \frac{F_x}{1/2 \rho U_C^2 T_m L_{PP}} \quad (5)$$

$$Y' = \frac{F_y}{1/2 \rho U_C^2 T_m L_{PP}} \quad (6)$$

$$N' = \frac{M_z}{1/2 \rho U_C^2 T_m L_{PP}^2} \quad (7)$$

For static tests, average values of surge and sway forces and yaw moment are computed from the time histories. For the dynamic tests, first the inertia forces and moment of the model ship and the mount are subtracted from the measured forces and moment, respectively. Then, the resultant time histories of the forces


and yaw moment are reconstructed with a 6th-order FS equation using the input PMM frequency as the prime frequency of the FS. Uncertainties related to the averaging and FS reconstruction processes are not considered in the present procedure.

2.3 Measurement Systems and Procedures

Three forces and three moments are measured with an Izumi six-component strain-gage type load cell, six Izumi amplifiers, 16-channel AD converter and PC. Maximum force and moment ranges are 500 N for F_x , F_y , F_z and 50 N-m, 50 N-m, 200 N-m for M_x , M_y , M_z , respectively.

Ship model motions are measured using a Krypton Electronic Engineering Rodym DMM motion tracker. The Rodym DMM is a camera-based measurement system that triangulates the position of a target in 3D space for contactless measurement and evaluation of 6DOF motions. The hardware consists of a camera module comprising three fixed CCD cameras, target with 1-256 light-emitting diodes (LED's), camera control unit, hand-held probe with six LED's, and PC. Krypton software is used for system calibration, and data acquisition and reduction.

Carriage speed is measured with an IIHR-designed and built speed circuit. The operating principle is integer pulse counting at a wheel-mounted encoder. The hardware consists of an 8000-count optical encoder, carriage wheel, sprocket pair and chain, analog-digital (AD) converter, and PC. Linear resolution of the encoder, sprocket pair and chain, and wheel assembly is 0.15 mm/pulse. The speed circuit is periodically bench-calibrated to determine

 INTERNATIONAL TOWING TANK CONFERENCE	ITTC – Recommended Procedures and Guidelines	7.5-02 06-04 Page 6 of 25	
	Forces and moment Uncertainty Analysis, Example for Planar Motion Mechanism Test	Effective Date 2008	Revision 00

and adjust the frequency input/voltage output transfer function.

A four-wheel carriage supports the main PMM mechanical system which is towed behind the IIHR drive carriage. The mechanical system is a scotch-yoke type which converts rotational motion of an 11 kW AC servo motor to linear sway motion of a sway box and angular yaw motion of a yaw platter beneath the sway box (See Figure 2). The scotch yoke is driven through a control rack, PC, and software up to 0.25 Hz with maximum sway and yaw amplitudes of ± 500 mm and $\pm 30^\circ$, respectively. A strongback (1.5 m) is attached to the yaw platter, which is pre-settable at a drift angle between $\pm 30^\circ$ for static drift or combined yaw and drift tests. Factory calibrated linear and rotational potentiometers are installed on the carriage to monitor and report the sway and yaw position of the sway box and yaw platter, respectively.

For static drift tests, the ship motion is defined by the towing speed U_C and the specified drift angle β relative to the towing direction. For dynamic tests, the ship motion is imposed to control velocities (surge u , sway v , yaw r), and accelerations (surge \dot{u} , sway \dot{v} , yaw \dot{r}) in the local ship coordinate system at any given instant (See figure 3).

Dynamic test ship motions are composed of:

- 1) carriage speed, U_C ;
- 2) PMM-generated transverse oscillation of the model from side to side (perpendicular to the towing direction) defined by the velocity v_{PMM} and the acceleration \dot{v}_{PMM} ;
- 3) PMM-generated horizontal rotation from side to side of the model around a vertical axis through the mid ship, defined by the

angular velocity r_{PMM} and the angular acceleration \dot{r}_{PMM} and

- 4) a drift angle β if the yaw and drift condition is considered (Fig. 2). The time-dependent PMM motion parameters can differ from facility to facility, but those for the current example are described basically by three quantities. These include the sway crank amplitude S_{mm} , yaw motion amplitude ψ_0 , and PMM frequency $\omega = 2\pi Nt/60$, where N is the number of PMM rotations per minute. The following relations are used to setup static and dynamic tests according to the test conditions in Tables 2-5:

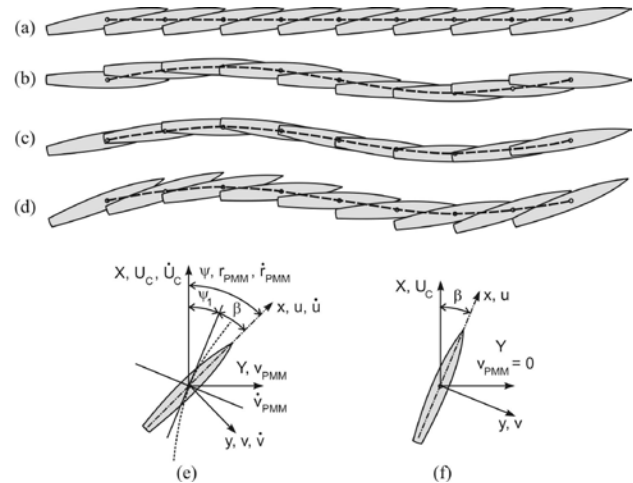



Figure 3 Definitions of PMM tests and motion parameters: (a) static drift; (b) pure sway; (c) pure yaw; (d) yaw and drift; (e) dynamic test motion parameters; (f) static test motion parameters.

Heading:

$$\psi = -\psi_0 \cos \omega t + \beta \quad (8)$$

Yaw rate:

$$r_{PMM} = -\psi_0 \omega \sin \omega t \quad (9)$$

 INTERNATIONAL TOWING TANK CONFERENCE	ITTC – Recommended Procedures and Guidelines	7.5-02 06-04 Page 7 of 25	
	Forces and moment Uncertainty Analysis, Example for Planar Motion Mechanism Test	Effective Date 2008	Revision 00

Yaw acceleration:

$$\dot{r}_{PMM} = -\psi_0 \omega^2 \cos \omega t \quad (10)$$

Transverse translation:

$$\eta_{PMM} = -2S_{mm} \sin \omega t \quad (11)$$

Transverse velocity:

$$v_{PMM} = -2\omega S_{mm} \cos \omega t \quad (12)$$

Transverse acceleration:

$$\dot{v}_{PMM} = 2\omega^2 S_{mm} \sin \omega t \quad (13)$$

where, η_{PMM} in (11) is the transverse position of the model ship in towing tank coordinates. If a different PMM motion generation mechanism is used, equations (8) to (13) should be replaced with the appropriate PMM motion equations.

The motion parameters of the model ship moving in a ship-fixed moving frame of reference can be expressed with the above PMM motion parameters. The carriage acceleration is assumed to be zero, i.e. $\dot{U}_C = 0$ in the following equations.

Sway velocity:

$$v = v_{PMM} \cos \psi - U_C \sin \psi \quad (14)$$

Sway acceleration:

$$\dot{v} = \dot{v}_{PMM} \cos \psi - r(U_C \cos \psi + v_{PMM} \sin \psi) \quad (15)$$

Yaw rate:

$$r = r_{PMM} \quad (16)$$

Yaw acceleration:

$$\dot{r} = \dot{r}_{PMM} \quad (17)$$

Surge velocity:

$$u = U_C \cos \psi + v_{PMM} \sin \psi \quad (18)$$

Surge acceleration:

$$\dot{u} = \dot{v}_{PMM} \sin \psi + r(v_{PMM} \cos \psi - U_C \sin \psi) \quad (19)$$

2.4 Uncertainty Analysis

The Uncertainty analysis procedures are based on estimates of systematic bias (B) and random precision (P) limits, and their root-sum-square (RSS) combination to ascertain total uncertainty (U). UA is applied to data reduction equations (2) – (4) for dynamic tests and (5) – (7) for static tests, respectively, which are written in functional forms below (20) – (22) for dynamic tests and (23) – (25) for static tests, respectively.

$$X' = X' \left(L_{PP}, T_m, x_G, y_G, m, \rho, \right. \\ \left. u, v, r, \dot{u}, \dot{v}, \dot{r}, F_x \right) \quad (20)$$

$$Y' = Y' \left(L_{PP}, T_m, x_G, y_G, m, \rho, \right. \\ \left. u, v, r, \dot{v}, \dot{r}, F_y \right) \quad (21)$$

$$N' = N' \left(L_{PP}, T_m, x_G, y_G, m, I_z, \rho, \right. \\ \left. u, v, r, \dot{u}, \dot{v}, \dot{r}, M_z \right) \quad (22)$$

$$X' = X'(L_{PP}, T_m, \rho, U_C, F_x) \quad (23)$$

$$Y' = Y'(L_{PP}, T_m, \rho, U_C, F_y) \quad (24)$$

$$N' = N'(L_{PP}, T_m, \rho, U_C, M_z) \quad (25)$$

Bias limits are estimated with consideration of elemental error sources for individual variables, whereas precision limits are estimated end to end. Ninety-five percent confidence levels are achieved through careful estimation of bias errors and usage of a large sample, multiple test approach for precision errors. An error propagation diagram for PMM tests is shown in Figure 4.

2.4.1 Bias Limit

Fourteen elemental biases B_x , where $x = L_{PP}, T_m, x_G, y_G, m, I_z, \rho, u, v, r, \dot{u}, \dot{v}, \dot{r}, F$ (hereafter F is either F_x, F_y , or M_z) are identified from the error propagation equations of the DRE's (20) – (22) for dynamic tests, and five

elemental biases B_x , where $x = L_{PP}, T_m, \rho, U_C, F$ from (23) – (25) for static tests.

$$B_R^2 = \sum_x \theta_x^2 B_x^2 \quad (26)$$

Sensitivity coefficients $\theta_x = \partial R / \partial x$ (hereafter R is either X', Y' , or N') of individual variable results are evaluated analytically, and their definitions are summarized in Tables 12, 13, and 14 for $B_{X'}$, $B_{Y'}$, and $B_{N'}$, respectively. The individual bias limits B_x are defined and estimated as below. Additional or details of estimation procedures for some variables are presented in Appendices A, B, C, and D at the end of this procedure.

The model length bias limit is estimated as $B_{L_{PP}} = 0.002\text{m}$, which corresponds to 0.07% of L_{PP} , by assuming the model ship fabrication

error to be ± 1 mm in all coordinates according to ITTC Procedure 7.5-01-01-01 Rev 01, ‘Ship Models’.

B_{T_m} is composed of two uncorrelated elemental errors ($B_{T_m,1}, B_{T_m,2}$). $B_{T_m,1}$ is the marking accuracy of draft markers on the model ship surface, and assumed to be 0.1 mm. $B_{T_m,2}$ is from the model ship ballasting error with respect to the draft markers, which is estimated as 1 mm based on visual inspection. From the RSS of $B_{T_m,1}$ and $B_{T_m,2}$, B_{T_m} is estimated as 1 mm, which corresponds to 0.7% of T_m . The estimation procedure for the case of model ballasting based on displacement is given in Appendix A.

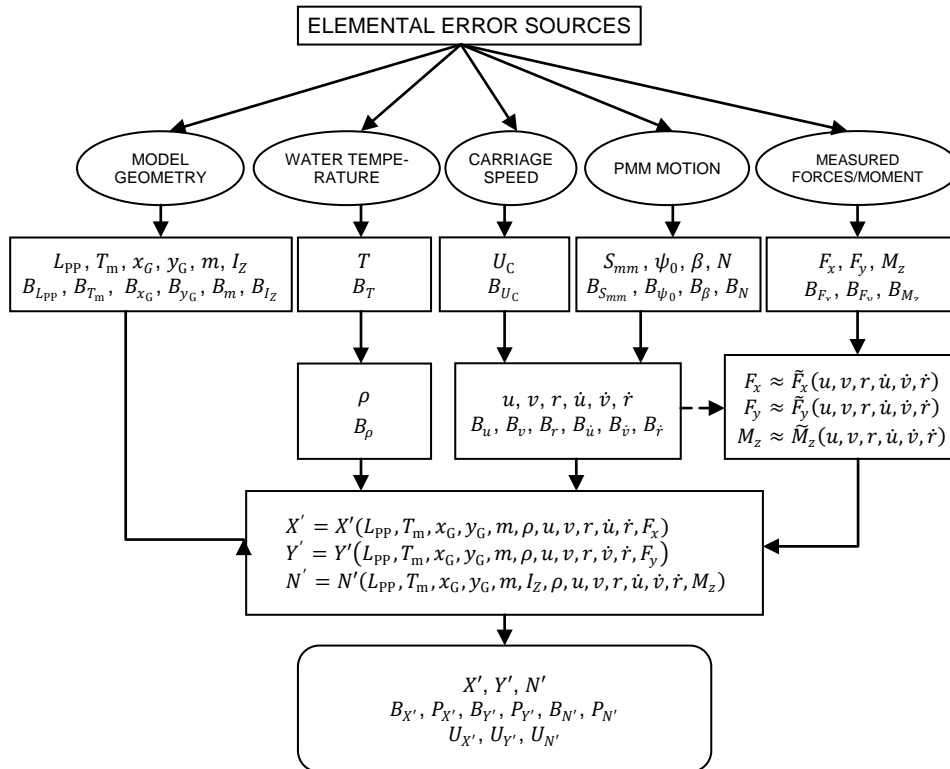



Figure 4 Propagation of experimental errors in a PMM test.

 INTERNATIONAL TOWING TANK CONFERENCE	ITTC – Recommended Procedures and Guidelines	7.5-02 06-04 Page 9 of 25	
	Forces and moment Uncertainty Analysis, Example for Planar Motion Mechanism Test	Effective Date 2008	Revision 00

The bias limits of COG (B_{x_G}, B_{y_G}) consist of two uncorrelated elemental errors; $B_{G,1}$ and $B_{G,2}$, where the subscript G represents either x_G or y_G . $B_{G,1}$ is the model installation error and $B_{G,2}$ is the deviation of actual model COG from the designed position. Estimated B_{x_G} and B_{y_G} are summarized as following:

Term (G)	$B_{G,1}$ [m]	$B_{G,2}$ [m]	B_G [m]
x_G	0.002	0.005	0.0054
y_G	0.001	0.002	0.0022

Total mass m of the model is calculated by summing individually measured element masses which are the bare model ship, ballast weights, and parts for model installation. Accordingly, B_m is the RSS of $B_{m,i}$'s which are the individual mass measurement errors. B_m is estimated as 0.11 kg (0.1% of $m=82.55$ kg). Measured masses of all elements together with their biases are summarized in Table 6.

From separate measurements of model ship yaw moment of inertia, B_{I_z} is estimated as 1.84 $\text{Kg}\cdot\text{m}^2$, which corresponds to 3.7 % of the measured model yaw moment of inertia $I_z = 49.79 \text{ kg}\cdot\text{m}^2$. Details of I_z measurement and B_{I_z} estimation procedures are given in Appendix B.

Water density is calculated from the ITTC 1963 density-temperature formula for fresh water.

$$\rho(T) = 999.784 + 0.0638 T - 0.00865 T^2 + 0.0000631 T^3 \quad (27)$$

Water temperature T is measured at the model mid draft with a resistive-type probe and

signal conditioner. The temperature-probe accuracy is rated at $B_T = \pm 0.2^\circ\text{C}$ and $B_\rho = \sqrt{(\partial\rho/\partial T)^2 B_T^2}$ is estimated as 0.041 kg/m^3 which is 0.004% of the measured water density $\rho = 998.1 \text{ kg/m}^3$ at 20°C .


No. (i)	Item	m_i [kg]	B_{m_i} [kg]
1	Bare model ship	55.99	0.045
2	Ballast weight 1	2.27	0.023
3	Ballast weight 6	2.27	0.023
4	Ballast weight 11	2.27	0.023
5	Ballast weight 12	2.27	0.023
6	Ballast weight 13	2.27	0.023
7	Ballast weight 15	1.70	0.023
8	Ballast weight 16	1.70	0.023
9	Ballast weight 18	1.13	0.023
10	Ballast weight 19	1.09	0.023
11	Ballast weight 23	1.13	0.023
12	Ballast weight 24	0.88	0.023
13	Ballast weight A	0.20	0.023
14	Ballast weight B	0.20	0.023
15	Ballast weight C	1.36	0.023
16	Krypton target	2.47	0.023
17	Part 1	1.11	0.023
18	Part 2	1.11	0.023
19	Part 3	1.11	0.023

$$m = \sum_i m_i = 82.55 \text{ Kg}$$

$$B_m = \sqrt{\sum_i B_{m_i}^2} = 0.11 \text{ Kg}$$

Table 6 Model mass bias estimation.

Carriage speed bias limit is estimated end-to-end by calibrating the carriage speed with respect to reference speeds. Reference speeds are obtained by measuring travel time Δt for a known distance ΔL . From the calibration B_{U_C} is estimated as 0.010m/s, which corresponds to 0.7% of carriage speed 1.531m/s ($Fr = 0.280$).

 INTERNATIONAL TOWING TANK CONFERENCE	ITTC – Recommended Procedures and Guidelines	7.5-02 06-04 Page 10 of 25	
	Forces and moment Uncertainty Analysis, Example for Planar Motion Mechanism Test	Effective Date 2008	Revision 00

Details of U_C calibration and B_{U_C} estimation procedures are summarized in Appendix C.

Bias limits of motion parameters $B_v, B_{\dot{v}}, B_r, B_{\dot{r}}, B_u, B_{\dot{u}}$ are estimated from error propagation equations (28) – (33) through their own DRE's (14) – (19), respectively.

$$B_v^2 = \theta_{U_C}^2 B_{U_C}^2 + \theta_{\psi}^2 B_{\psi}^2 + \theta_{v_{PMM}}^2 B_{v_{PMM}}^2 \quad (28)$$

$$B_{\dot{v}}^2 = \theta_{U_C}^2 B_{U_C}^2 + \theta_{\psi}^2 B_{\psi}^2 + \theta_r^2 B_r^2 + \theta_{v_{PMM}}^2 B_{v_{PMM}}^2 + \theta_{\dot{v}_{PMM}}^2 B_{\dot{v}_{PMM}}^2 \quad (29)$$

$$B_r^2 = \theta_{\psi_0}^2 B_{\psi_0}^2 + \theta_N^2 B_N^2 + \theta_t^2 B_t^2 \quad (30)$$

$$B_{\dot{r}}^2 = \theta_{\psi_0}^2 B_{\psi_0}^2 + \theta_N^2 B_N^2 + \theta_t^2 B_t^2 \quad (31)$$

$$B_u^2 = \theta_{U_C}^2 B_{U_C}^2 + \theta_{\psi}^2 B_{\psi}^2 + \theta_{v_{PMM}}^2 B_{v_{PMM}}^2 \quad (32)$$

$$B_{\dot{u}}^2 = \theta_{U_C}^2 B_{U_C}^2 + \theta_{\psi}^2 B_{\psi}^2 + \theta_r^2 B_r^2 + \theta_{v_{PMM}}^2 B_{v_{PMM}}^2 + \theta_{\dot{v}_{PMM}}^2 B_{\dot{v}_{PMM}}^2 \quad (33)$$

Of the additional biases, $B_{\psi}, B_{v_{PMM}}, B_{\dot{v}_{PMM}}$ are estimated from their DRE's (19), (23), (24), respectively.

$$B_{\psi}^2 = \theta_{\psi_0}^2 B_{\psi_0}^2 + \theta_N^2 B_N^2 + \theta_t^2 B_t^2 + \theta_{\beta}^2 B_{\beta}^2 \quad (34)$$

$$B_{v_{PMM}}^2 = \theta_N^2 B_N^2 + \theta_{S_{mm}}^2 B_{S_{mm}}^2 + \theta_t^2 B_t^2 \quad (35)$$

$$B_{\dot{v}_{PMM}}^2 = \theta_N^2 B_N^2 + \theta_{S_{mm}}^2 B_{S_{mm}}^2 + \theta_t^2 B_t^2 \quad (36)$$

The sensitivity coefficients in (28) – (36) are evaluated analytically. Of the five elemental errors associated with motion parameters B_x , where $x = S_{mm}, N, t, \beta, \psi_0$, $B_{S_{mm}}$ is from the test setup and B_N, B_t are from empirical estimation, which are presented in Table 7. Drift angle bias limit B_{β} is assumed to be composed of two uncorrelated elemental errors $B_{\beta,align}$ and $B_{\beta,drift}$. $B_{\beta,align}$ is the model ship installation error with respect to straight towing direction and assumed to be 0.03° . $B_{\beta,drift}$ is the

deviation from designated drift angle setting and estimated end-to-end by calibrating the drift angle with respect to reference angles, and estimated as 0.22° . Details of drift angle calibration and B_{β} estimation procedures are presented in the Appendix D. Bias limit of the maximum heading angle of yaw motion B_{ψ_0} is assumed to be same as B_{β} .

Uncertainty	Magnitude
$B_{S_{mm}}$	0.0005 m
$B_{\beta} = B_{\psi_0}$	0.22 deg
B_N	0.0006 rpm
B_t	0.001 sec

Table 7 Elemental uncertainties related to the PMM motion generation.

ε_{β} [rad]	ε_{align} [rad]	$\beta = -10^\circ$		
3.84×10^{-3}	5.24×10^{-4}	$\frac{dF_x}{d\beta}$	$B_{F_x,\beta}$	$B_{F_x,align}$
		[N/rad]	[N]	[N]
		30.2	0.1161	0.0158
		$\frac{dF_y}{d\beta}$	$B_{F_y,\beta}$	$B_{F_y,align}$
		[N/rad]	[N]	[N]
		209.9	0.8061	0.1100
$\frac{dM_z}{d\beta}$	$B_{M_z,\beta}$	$B_{M_z,align}$		
[Nm/rad]	[Nm]	[Nm]		
283.9	1.0903	0.1488		
$B_{F,\beta}^2 = \left(\frac{dF}{d\beta}\right)^2 \varepsilon_{\beta}^2, B_{F,align}^2 = \left(\frac{dF}{d\beta}\right)^2 \varepsilon_{F,align}^2 ;$ $F = F_x, F_y, \text{ or } M_z$				

Table 8 $B_{F,\beta}$ and $B_{F,align}$ estimations.

Bias limits of measured forces/moment B_F , where F is either F_x , F_y , or M_z , is composed of 9 uncorrelated element errors for dynamic tests

$$B_F^2 = B_{F,calib}^2 + B_{F,acquis}^2 + B_{F,u}^2 + B_{F,\dot{u}}^2 + B_{F,v}^2 + B_{F,\dot{v}}^2 + B_{F,r}^2 + B_{F,\dot{r}}^2 + B_{F,t}^2 \quad (37)$$

and 4 uncorrelated element errors for static tests.

$$B_F^2 = B_{F,\beta}^2 + B_{F,align}^2 + B_{F,calib}^2 + B_{F,acquis}^2 \quad (38)$$

$B_{F,\beta}$ and $B_{F,align}$ are from drift angle setting error and mis-alignment of model ship with respect to straight towing direction, respectively. Estimation procedures and results of $B_{F,\beta}$ and $B_{F,align}$ are summarized in Table 8. Sensitivity coefficients $\partial F/\partial \beta$'s are obtained from static drift test results. $B_{F,calib}$ is the RSS of the errors of individual weights used for forces/moment gauge calibration. Estimation procedures and measurement results of $B_{F,calib}$ are summarized in Table 9.

F_x		F_y	
weight, w_i [N]	$\varepsilon_{w,i}$ [N]	weight, w_i [N]	$\varepsilon_{w,i}$ [N]
9.81	0.00020	4.90	0.00010
14.71	0.00029	9.81	0.00020
19.61	0.00039	14.71	0.00029
49.03	0.00098	19.61	0.00039
-	-	49.03	0.00098

$$B_{F,calib} = \sqrt{\sum_i \varepsilon_{w,i}^2}$$

$$B_{F_x,calib} = B_{F_y,calib} = 0.001N$$

Table 9a $B_{F_x,calib}$ and $B_{F_y,calib}$ estimation.

weight, w_i [N]	$M_{z,calib,i}$ [Nm]	ε_{w_i} [N]	$B_{M_z,calib,i}$ [Nm]
4.90	2.24	0.00010	0.00245
9.81	4.48	0.00020	0.00490
14.71	6.73	0.00029	0.00736
19.61	8.97	0.00039	0.00981
49.03	22.42	0.00098	0.02452

$$L_{calib} = 0.4572m, \varepsilon_{L_{calib}} = 0.0005m$$

$$M_{z,calib,i} = w_i \times L_{calib}$$

$$B_{M_z,calib,i}^2 = \left(\frac{\partial M_{z,calib,i}}{\partial w_i}\right)^2 \varepsilon_{w_i}^2 + \left(\frac{\partial M_{z,calib,i}}{\partial L_{calib}}\right)^2 \varepsilon_{L_{calib}}^2$$

$$= L_{calib}^2 \varepsilon_{w_i}^2 + \varepsilon_{w_i}^2 \varepsilon_{L_{calib}}^2$$

$$B_{M_z,calib} = \sqrt{\sum_i B_{M_z,calib,i}^2} = 0.028Nm$$

Table 9b $B_{M_z,calib}$ estimation.

F_x		F_y		M_z	
$ F_x $ [N]	$ \overline{\Delta F_x} _{max}$ [N]	$ F_y $ [N]	$ \overline{\Delta F_y} _{max}$ [N]	$ M_z $ [Nm]	$ \overline{\Delta M_z} _{max}$ [Nm]
9.81	0.0282	9.81	0.0262	8.97	0.0352
14.71	0.0407	19.61	0.0558	14.93	0.0494
19.61	0.0571	39.23	0.1334	26.90	0.0782
29.42	0.0769	58.84	0.2009	35.87	0.1045
49.03	0.1326	78.45	0.2767	44.84	0.1389

$$|\overline{\Delta F}|_{max} = |\overline{\Delta F}| + P_{|\Delta F|}$$

$$P_{|\Delta F|} = \frac{2S_{|\Delta F|}}{\sqrt{M}}, S_{|\Delta F|} = \left[\sum_{i=1}^M \frac{(|\Delta F_i| - |\overline{\Delta F}|)^2}{M-1} \right]^{\frac{1}{2}}$$

$$\overline{\Delta F} = \frac{1}{M} \sum_{i=1}^M |\Delta F_i|, \Delta F_i = F_{measured,i} - F_{applied,i}$$


M : number of repeat = 12

$$B_{F_x,acquis} = 0.002634|F_x| + 0.002534$$

$$B_{F_y,acquis} = 0.003668|F_y| + 0.001245$$

$$B_{M_z,acquis} = 0.002927|M_z| + 0.002505$$

Table 10 $B_{F,acquis}$ estimation.

 INTERNATIONAL TOWING TANK CONFERENCE	ITTC – Recommended Procedures and Guidelines	7.5-02 06-04 Page 12 of 25	
	Forces and moment Uncertainty Analysis, Example for Planar Motion Mechanism Test	Effective Date 2008	Revision 00

$B_{F,acquis}$ is from the volt-to-force conversion error of the forces/moment measurement gauges. Estimation procedures and measurement results of $B_{F,acquis}$ are summarized in Table 10. Other elemental bias errors $B_{F,u}$, $B_{F,\dot{u}}$, $B_{F,v}$, $B_{F,\dot{v}}$, $B_{F,r}$, $B_{F,\dot{r}}$, $B_{F,t}$ are calculated by applying the error propagation equation to measured forces and moment F by assuming F is a function of motion parameters (u , v , r , \dot{u} , \dot{v} , \dot{r}) and time (t),

$$B_{F,x} = \frac{\partial F}{\partial x} B_x \quad (39)$$

where $x = u$, v , r , \dot{u} , \dot{v} , \dot{r} , t .

Pure yaw	$\begin{aligned} \tilde{F}_x &= X_0 + X_u u + X_r r + X_{rr} r^2 + X_{\dot{u}} \dot{u} + X_{\dot{r}} \dot{r} \\ &\quad + X_v v + X_{\dot{v}} \dot{v} \\ \tilde{F}_y &= Y_0 + Y_u u + Y_r r + Y_{rrr} r^3 + Y_{\dot{u}} \dot{u} + Y_{\dot{r}} \dot{r} \\ &\quad + Y_v v + Y_{\dot{v}} \dot{v} \\ \tilde{M}_z &= M_0 + M_u u + M_r r + M_{rrr} r^3 + M_{\dot{u}} \dot{u} + M_{\dot{r}} \dot{r} \\ &\quad + M_v v + M_{\dot{v}} \dot{v} \end{aligned}$
Pure sway	$\begin{aligned} \tilde{F}_x &= X_0 + X_u u + X_r r + X_{\dot{u}} \dot{u} + X_{\dot{r}} \dot{r} \\ &\quad + X_v v + X_{\dot{v}} \dot{v} + X_{vv} v^2 \\ \tilde{F}_y &= Y_0 + Y_u u + Y_r r + Y_{\dot{u}} \dot{u} + Y_{\dot{r}} \dot{r} \\ &\quad + Y_v v + Y_{\dot{v}} \dot{v} + Y_{v v} v v \\ \tilde{M}_z &= M_0 + M_u u + M_r r + M_{\dot{u}} \dot{u} + M_{\dot{r}} \dot{r} \\ &\quad + M_v v + M_{\dot{v}} \dot{v} + M_{v v} v v \end{aligned}$
Yaw and drift	$\begin{aligned} \tilde{F}_x &= X_0 + X_u u + X_r r + X_{rr} r^2 + X_{\dot{u}} \dot{u} + X_{\dot{r}} \dot{r} \\ &\quad + X_v v + X_{\dot{v}} \dot{v} + X_{uu} u^2 + X_{vv} v^2 + X_{uv} uv \\ \tilde{F}_y &= Y_0 + Y_u u + Y_r r + Y_{rrr} r^3 + Y_{\dot{u}} \dot{u} + Y_v v + Y_{vu} vu \\ &\quad + Y_{v v} v v + Y_{v r} v r + Y_{r v} r v \\ &\quad + Y_{rvv} rvv + Y_{vrr} vrr \\ \tilde{M}_z &= M_0 + M_u u + M_r r + M_{rrr} r^3 + M_{\dot{u}} \dot{u} \\ &\quad + M_v v + M_{vu} vu + M_{rvv} rvv + M_{vrr} vrr \\ &\quad + M_{v v} v v + M_{v r} v r + M_{r v} r v \end{aligned}$

Table 11 Definitions of polynomial models.

Due to the absence of DRE with respect to those variables, measured forces/moment F is approximated as a polynomial expansion model \tilde{F} of the variables.

$$F \approx \tilde{F} = \sum_k \sum_{n=1}^J A_{k,n} (x_k)^n \quad (40)$$

where, $n=0, 1, \dots, J$; $x_k = u, v, r, \dot{u}, \dot{v}, \dot{r}$; $A_{k,n}$ is the constant coefficient of n^{th} order x_k variable which is a function of time t . The number of variables k employed and/or the highest order J of each variable varies with each force component and type of test. The polynomial model definition for all forces/moment components for all test types of the UA test cases are summarized in Table 11.


With the polynomial modeling of the measured forces or moment the bias limits in the equation (39) are evaluated

$$B_{F,x} = \frac{\partial F}{\partial x} B_x \approx \frac{\partial \tilde{F}}{\partial x} B_x \quad (41)$$

The coefficients of each polynomial model are calculated with the Least-Square fitting method. In equations (39) and (41) the elemental bias limits B_v , $B_{\dot{v}}$, B_r , $B_{\dot{r}}$, B_u , $B_{\dot{u}}$ are identical with the bias limits defined in (28) to (33), respectively. With respect to $B_{F,t}$, the sensitivity coefficient $\partial F / \partial t$ is calculated numerically from the measured time histories of F .

2.4.2 Precision Limit

The precision limits are determined from 12 repeat tests. The datasets are spaced in time at least 12 minutes between tests to minimize flow disturbances from previous runs, while spanning over a time period, usually one day, that is large relative to time scales of the factors that influence variability of the measurements. The same model ship, PMM motion

 INTERNATIONAL TOWING TANK CONFERENCE	ITTC – Recommended Procedures and Guidelines	7.5-02 06-04 Page 13 of 25	
	Forces and moment Uncertainty Analysis, Example for Planar Motion Mechanism Test	Effective Date 2008	Revision 00

generator, load cell, and motion tracker are used for the repeat tests due to limitations of time and experiment resources. The model is not dismantled and re-installed during the repeat tests. However, the PMM motion control parameters, such as drift angle, sway crank amplitude, or maximum heading angle settings are changed between tests. The precision limits are computed with the standard multiple-test equation

$$P_{\bar{R}} = \frac{tS_{\bar{R}}}{\sqrt{12}} \quad (42)$$

where $R = X', Y', N'$ and $t=2$ is the coverage factor for 95% confidence level. $S_{\bar{R}}$ is the standard deviation defined as

$$S_{\bar{R}} = \left[\sum_{k=1}^{12} \frac{(R_k - \bar{R})^2}{11} \right]^{\frac{1}{2}} \quad (43)$$

and

$$\bar{R} = \frac{1}{12} \sum_{k=1}^{12} R_k \quad (44)$$


where, R_k is either $X', Y',$ or N' of the k^{th} run, which are defined in (2) – (4) for dynamic tests and (5) – (7) for static tests, respectively.

2.4.3 UA Results

Uncertainty assessment results are presented in Table 15 for static drift tests and Tables 16 - 18 for dynamic tests. Each table consists of three parts; DRE variables and their error contributions to the total bias limit of non-dimensional forces and moment B_R (top), bias limit of measured forces and moments B_F including contributions from elemental bias errors $B_{F,x}$ (middle), and total bias B_R and precision P_R limits, and their contributions to total uncertainty U_R (bottom). The latter includes scaled total uncertainties in percentile of either

variable magnitude or its dynamic range. For dynamic tests the UA results only at their maximum motions are presented and compared in the tables.

Static tests From Table 15 (top) the largest bias is the carriage speed B_{U_C} and the second largest bias is the measured force B_F for X' , while B_F is the largest bias and B_{U_C} is the second largest bias for Y' and N' . The mean draft bias B_{T_m} contributes rather large 16% to $B_{X'}$, while small $< 5\%$ to $B_{Y'}$ and $B_{N'}$. Water density B_ρ and model length $B_{L_{pp}}$ are small $< 0.5\%$ or negligibly contributing to the total bias B_R . The measured forces/moment bias B_F , a common large bias for X', Y', N' , is mainly from drift angle error $B_{F,\beta}$ as presented in Table 15 (middle). $B_{F,\beta}$ contributes over 90% to B_F for all cases. Other elemental biases of B_F ($B_{F,\text{align}}, B_{F,\text{calib}}, B_{F,\text{acquis}}$) contribute small or negligibly to B_F . From Table 15 (bottom), the total bias limit B_R contributes over 90%, and the precision limit P_R contributes less than 10% to U_R , indicating most DRE variable results are highly repeatable. Total uncertainties U_R 's are reasonably small, 1.9%, 3.4%, and 2.8% of $X', Y',$ and N' , respectively, but relatively large compared with the resistance test uncertainty $U_{C_T} = 0.67\%$ of C_T reported in the ITTC Procedure 7.5-02-02-02 Rev01, 'Uncertainty Analysis, Example for Resistance Test.' Although the static drift tests are similar with the resistance test, a steady straight towing test, additional errors from the drift angle setting associated with static drift test might explain the higher uncertainty levels. Improvements of static drift test uncertainty can be achieved by improving the carriage speed control for X' and drift angle setting accuracy for Y' and N' , which are the biggest bias error sources.

	ITTC – Recommended Procedures and Guidelines	7.5-02 06-04 Page 14 of 25	
	Forces and moment Uncertainty Analysis, Example for Planar Motion Mechanism Test	Effective Date 2008	Revision 00


Dynamic tests For pure yaw tests (Table 16), the primary bias is surge velocity B_u and the secondary is measured forces/moment B_F for X' , B_F is the primary bias and the yaw rate B_r is secondary bias for Y' , and again B_F is the primary and B_u is the secondary biases for N' , respectively. The mean draft B_{T_m} contributes 4% to $B_{X'}$, 0.6% to $B_{Y'}$, and 8% to $B_{N'}$, respectively. The longitudinal COG B_{x_G} contributes 3% only to $B_{N'}$, the sway velocity B_v contributes 4% only to $B_{X'}$, and the sway acceleration $B_{\dot{v}}$ contributes 4% only to $B_{N'}$, respectively, otherwise negligible. $B_{L_{pp}}$, B_{y_G} , B_m , B_{I_z} , B_ρ are negligible for all cases. The measured forces/moment bias B_F is composed largely of surge velocity $B_{F,u}$ and acceleration $B_{F,\dot{u}}$ for F_x , and of the yaw rate $B_{F,r}$ for F_y and M_z , respectively. Other elemental biases of B_F ($B_{F,calib}$, $B_{F,acquis}$, $B_{F,v}$, $B_{F,\dot{v}}$, $B_{F,\dot{r}}$, $B_{F,t}$) are small $< 10\%$ or maybe negligible contributions. The precision error $P_{X'}$ is dominant 75% for X' , but the total bias errors $B_{Y'}$ and $B_{N'}$ are dominant $> 90\%$ for Y' and N' . The total uncertainty $U_{X'}$ is 8% of X' , and $U_{Y'}$ and $U_{N'}$ are 5%, and 1.4% of the dynamic ranges of Y' and N' , respectively.

For pure sway test (Table 17), the surge velocity B_u is the primary bias and measured force B_F and mean draft B_{T_m} are secondary biases for X' , B_F is the primary bias and B_u is the secondary bias for Y' and N' , respectively. $B_{L_{pp}}$, B_{x_G} , B_{y_G} , B_m , B_{I_z} , B_ρ , B_v , B_r , $B_{\dot{u}}$, $B_{\dot{v}}$, $B_{\dot{r}}$ all contribute small or negligibly to B_R for all cases. The measured forces/moment bias B_F is composed mainly of the sway velocity $B_{F,v}$ for all F , but also from $B_{F,acquis}$ and $B_{F,u}$ for B_{F_x} . Other elemental biases of B_F ($B_{F,calib}$, $B_{F,r}$, $B_{F,\dot{u}}$, $B_{F,\dot{v}}$, $B_{F,\dot{r}}$, $B_{F,t}$) are negligible. Both the precision error $P_{X'}$ and the total bias error $B_{X'}$ contribute considerably to the total uncertainty

$U_{X'}$ for X' , while $B_{X'}$ is dominant $> 90\%$ for Y' and N' . $U_{X'}$ is 5.8% of X' , and $U_{Y'}$ and $U_{N'}$ are all 2.1% of the dynamic ranges of Y' and N' , respectively.

For yaw and drift tests (Table 18), the surge velocity B_u is the primary bias and the measured forces/moment B_F is the secondary bias for X' , B_F is the primary and the yaw rate B_r is the secondary bias for Y' , and B_F is primary and B_u is the secondary bias for N' , respectively. $B_{L_{pp}}$, B_{T_m} , B_{x_G} , B_{y_G} , B_m , B_{I_z} , B_ρ , B_v , $B_{\dot{v}}$, $B_{\dot{r}}$ all contribute small or negligibly to B_R for all cases. The measured forces/moment bias B_F is composed largely of $B_{F,u}$, $B_{F,\dot{u}}$, $B_{F,r}$ for F_x , and $B_{F,v}$, $B_{F,r}$ for F_y and M_z . Other elemental biases of B_F ($B_{F,calib}$, $B_{F,acquis}$, $B_{F,\dot{v}}$, $B_{F,\dot{r}}$, $B_{F,t}$) are negligible. The precision error $P_{X'}$ and the total bias error $B_{X'}$ are both significant to $U_{X'}$, while the bias errors $B_{Y'}$ and $B_{N'}$ are dominant for Y' and N' . The total uncertainty $U_{X'}$ is about 7% of X' , $U_{Y'}$ and $U_{N'}$ are 3.6% and 1.5% of the dynamic ranges of Y' and N' , respectively.

In conclusion for the dynamic tests, primary biases vary according to type of the test while the measured forces/moment bias error B_F is the common largest bias. Ship model geometry related bias errors and water density bias are contributing small or negligibly to the total bias limit B_R except for the mean draft bias B_{T_m} and the longitudinal COG bias B_{x_G} . However, the errors from motion parameters and measured forces/moment are dominant according to forces/moment component and test type. Bias limit dominates over the precision limit for Y' and N' , but not for X' . The total uncertainties U_R 's are varying 6% ~ 8% of X' , 1% ~ 5% of Y' and N' according to test type, which are larger than those of the static drift test results. Of

	ITTC – Recommended Procedures and Guidelines	7.5-02 06-04 Page 15 of 25	
	Forces and moment Uncertainty Analysis, Example for Planar Motion Mechanism Test	Effective Date 2008	Revision 00

the four different types of dynamic PMM tests, the pure yaw test total uncertainty is relatively higher than other kinds of PMM tests. Dynamic test results can be improved by improving carriage speed control to reduce the bias limit and increasing the number of repeat to reduce the precision limit for X' , and by improving the PMM motion control to reduce the bias limit for Y' and N' , respectively.

3. REFERENCES

Benedetti, L., Bouscasse, B., Broglia, R., Fab-
bri, L., La Gala, F., and Lugni, C., 2006,
“PMM Model Test with DDG51 Including

Uncertainty Assessment,” INSEAN Report
No. 14, 174 pp.

Simonsen, C., 2004, “PMM Model Test with
DDG51 Including Uncertainty Assessment,”
Force Technology Report No. ONR1187
01, 145 pp.

Yoon, H.-S., Longo, J., Toda, Y., and Stern, F.,
2007, “PMM Tests and Uncertainty As-
sessment for Surface Combatant Including
Comparisons Between Facilities,” IIHR –
Hydroscience & Engineering Report No.
####, ## pp.

	Dynamic Tests	Static Tests
θ_{F_x}	$\frac{2}{\rho(u^2+v^2)T_m L_{PP}}$	$\frac{2}{\rho U_C^2 T_m L_{PP}}$
θ_ρ	$\frac{-2(F_x+m(\dot{u}-rv-x_G r^2-y_G \dot{r}))}{\rho^2(u^2+v^2)T_m L_{PP}}$	$\frac{-2F_x}{\rho^2 U_C^2 T_m L_{PP}}$
θ_{T_m}	$\frac{-2(F_x+m(\dot{u}-rv-x_G r^2-y_G \dot{r}))}{\rho(u^2+v^2)T_m^2 L_{PP}}$	$\frac{-2F_x}{\rho U_C^2 T_m^2 L_{PP}}$
$\theta_{L_{PP}}$	$\frac{-2(F_x+m(\dot{u}-rv-x_G r^2-y_G \dot{r}))}{\rho(u^2+v^2)T_m L_{PP}^2}$	$\frac{-2F_x}{\rho U_C^2 T_m L_{PP}^2}$
θ_{U_C}	-	$\frac{-4F_x}{\rho U_C^3 T_m L_{PP}}$
θ_m	$\frac{2(\dot{u}-rv-x_G r^2-y_G \dot{r})}{\rho(u^2+v^2)T_m L_{PP}}$	-
θ_{x_G}	$\frac{-2mr^2}{\rho(u^2+v^2)T_m L_{PP}}$	-
θ_{y_G}	$\frac{-2m\dot{r}}{\rho(u^2+v^2)T_m L_{PP}}$	-
θ_u	$\frac{-4u(F_x+m(\dot{u}-rv-x_G r^2-y_G \dot{r}))}{\rho(u^2+v^2)^2 T_m L_{PP}}$	-
$\theta_{\dot{u}}$	$\frac{-2m}{\rho(u^2+v^2)T_m L_{PP}}$	-
θ_v	$\frac{2}{\rho(u^2+v^2)T_m L_{PP}} \left[-mr - \frac{2v(F_x+m(\dot{u}-rv-x_G r^2-y_G \dot{r}))}{(u^2+v^2)} \right]$	-
θ_r	$\frac{-2m(v+2x_G r)}{\rho(u^2+v^2)T_m L_{PP}}$	-
$\theta_{\dot{r}}$	$\frac{-2my_G}{\rho(u^2+v^2)T_m L_{PP}}$	-

Table 12 Definitions of sensitivity coefficients for B_X .

	Dynamic Tests	Static Tests
θ_{F_y}	$\frac{2}{\rho(u^2+v^2)T_m L_{PP}}$	$\frac{2}{\rho U_C^2 T_m L_{PP}}$
θ_ρ	$\frac{-2(F_y + m(\dot{v} + ru - y_G r^2 + x_G \dot{r}))}{\rho^2(u^2+v^2)T_m L_{PP}}$	$\frac{-2F_y}{\rho^2 U_C^2 T_m L_{PP}}$
θ_{T_m}	$\frac{-2(F_y + m(\dot{v} + ru - y_G r^2 + x_G \dot{r}))}{\rho(u^2+v^2)T_m^2 L_{PP}}$	$\frac{-2F_y}{\rho U_C^2 T_m^2 L_{PP}}$
$\theta_{L_{PP}}$	$\frac{-2(F_y + m(\dot{v} + ru - y_G r^2 + x_G \dot{r}))}{\rho(u^2+v^2)T_m L_{PP}^2}$	$\frac{-2F_y}{\rho U_C^2 T_m L_{PP}^2}$
θ_{U_C}	-	$\frac{-4F_y}{\rho U_C^3 T_m L_{PP}}$
θ_m	$\frac{2(\dot{v} + ru - y_G r^2 + x_G \dot{r})}{\rho(u^2+v^2)T_m L_{PP}}$	-
θ_{x_G}	$\frac{2m\dot{r}}{\rho(u^2+v^2)T_m L_{PP}}$	-
θ_{y_G}	$\frac{-2mr^2}{\rho(u^2+v^2)T_m L_{PP}}$	-
θ_u	$\frac{2}{\rho(u^2+v^2)T_m L_{PP}} \left[mr - \frac{2u(F_y + m(\dot{v} + ru - y_G r^2 + x_G \dot{r}))}{(u^2+v^2)} \right]$	-
θ_v	$\frac{-4v(F_y + m(\dot{v} + ru - y_G r^2 + x_G \dot{r}))}{\rho(u^2+v^2)^2 T_m L_{PP}}$	-
$\theta_{\dot{v}}$	$\frac{2m}{\rho(u^2+v^2)T_m L_{PP}}$	-
θ_r	$\frac{2m(u - 2y_G r)}{\rho(u^2+v^2)T_m L_{PP}}$	-
$\theta_{\dot{r}}$	$\frac{2mx_G}{\rho(u^2+v^2)T_m L_{PP}}$	-

Table 13 Definitions of sensitivity coefficients for \mathbf{B}_Y .

	Dynamic Tests	Static Tests
θ_{M_z}	$\frac{2}{\rho(u^2+v^2)T_m L_{PP}^2}$	$\frac{2}{\rho U_C^2 T_m L_{PP}^2}$
θ_{ρ}	$\frac{-2(M_z + I_z \dot{r} + m(x_G(\dot{v} + ru) - y_G(\dot{u} - rv)))}{\rho^2(u^2+v^2)T_m L_{PP}^2}$	$\frac{-2M_z}{\rho^2 U_C^2 T_m L_{PP}^2}$
θ_{T_m}	$\frac{-2(M_z + I_z \dot{r} + m(x_G(\dot{v} + ru) - y_G(\dot{u} - rv)))}{\rho(u^2+v^2)T_m^2 L_{PP}^2}$	$\frac{-2M_z}{\rho U_C^2 T_m^2 L_{PP}^2}$
$\theta_{L_{PP}}$	$\frac{-4(M_z + I_z \dot{r} + m(x_G(\dot{v} + ru) - y_G(\dot{u} - rv)))}{\rho(u^2+v^2)T_m L_{PP}^3}$	$\frac{-4M_z}{\rho U_C^2 T_m L_{PP}^3}$
θ_{U_C}	-	$\frac{-4M_z}{\rho U_C^3 T_m L_{PP}^2}$
θ_{I_z}	$\frac{2\dot{r}}{\rho(u^2+v^2)T_m L_{PP}^2}$	-
θ_m	$\frac{2(x_G(\dot{v} + ru) - y_G(\dot{u} - rv))}{\rho(u^2+v^2)T_m L_{PP}^2}$	-
θ_{x_G}	$\frac{2m(\dot{v} + ru)}{\rho(u^2+v^2)T_m L_{PP}^2}$	-
θ_{y_G}	$\frac{-2m(\dot{u} - rv)}{\rho(u^2+v^2)T_m L_{PP}^2}$	-
θ_u	$\frac{2}{\rho(u^2+v^2)T_m L_{PP}^2} \left[mx_G r - \frac{2u(M_z + I_z \dot{r} + m(x_G(\dot{v} + ru) - y_G(\dot{u} - rv)))}{(u^2+v^2)} \right]$	-
$\theta_{\dot{u}}$	$\frac{-2my_G}{\rho(u^2+v^2)T_m L_{PP}^2}$	-
θ_v	$\frac{2}{\rho(u^2+v^2)T_m L_{PP}^2} \left[my_G r - \frac{2v(M_z + I_z \dot{r} + m(x_G(\dot{v} + ru) - y_G(\dot{u} - rv)))}{(u^2+v^2)} \right]$	-
$\theta_{\dot{v}}$	$\frac{2mx_G}{\rho(u^2+v^2)T_m L_{PP}^2}$	-
θ_r	$\frac{2m(x_G u + y_G v)}{\rho(u^2+v^2)T_m L_{PP}^2}$	-
$\theta_{\dot{r}}$	$\frac{2I_z}{\rho(u^2+v^2)T_m L_{PP}^2}$	-

Table 14 Definitions of the sensitivity coefficients for $B_{N'}$.

R	Var. (x)	L_{pp}	T_m	ρ	U_C	F	
	Unit	m	m	kg/m ³	m/s	N,Nm	
	Mag.	3.048	0.132	998.1	1.531	-	
	B_x	0.002	0.001	0.041	0.011	-	
X'	$\frac{\theta_x^2 B_x^2}{B_R^2}$	0.1	15.8	0.0	49.4	34.7	
Y'	$\frac{B_x^2}{B_R^2}$	0.0	5.3	0.0	16.6	78.0	
X'	(%)	0.1	3.2	0.0	10.1	86.6	
F	$\frac{B_{F_x}^2}{B_F^2}$ (%)				B_F	F	$\frac{B_F}{ F }$
	β	align	calib	acquis	[N]	[N]	(%)
	F_x	91.8	1.7	0.0	6.5	0.122	10.9
F_y	97.0	1.8	0.0	1.2	0.826	28.5	2.9
M_z	96.8	1.8	0.1	1.4	1.118	44.1	2.5
R	B_R	$\frac{B_R^2}{U_R^2}$	P_R	$\frac{P_R^2}{U_R^2}$	U_R	R	$\frac{U_R}{ R }$
	[10 ⁻²]	(%)	[10 ⁻²]	(%)	[10 ⁻²]	[-]	(%)
	X'	0.045	96.6	0.008	3.4	0.045	0.023
Y'	0.201	95.1	0.046	4.9	0.206	0.061	3.4
N'	0.085	94.5	0.020	5.5	0.087	0.031	2.8

Table 15 UA summary of static drift test ($\beta = -10^\circ$).

R	Var. (x)	L_{pp}	T_m	x_G	y_G	m	I_z	ρ	u	v	r	\dot{u}	\dot{v}	\dot{r}	F
	Unit	m	m	m	m	kg	kgm ²	kg/m ³	m/s	m/s	rad/s	m/s ²	m/s ²	rad/s ²	N,Nm
	Mag.	3.048	0.132	-0.016	0.000	82.55	49.79	998.1	1.527	0.002	0.150	0.000	0.003	0.000	-
	B_x	0.002	0.001	0.005	0.002	0.11	1.84	0.041	0.010	0.006	0.003	0.002	0.002	0.000	-
X'	$\frac{\theta_x^2 B_x^2}{B_R^2}$	0.0	4.0	0.1	0.0	0.0	-	0.0	67.6	3.7	0.0	11.0	-	0.0	13.5
Y'	$\frac{B_x^2}{B_R^2}$	0.0	0.6	0.0	0.0	0.1	-	0.0	9.0	0.0	27.1	-	3.2	0.0	60.0
N'	(%)	0.0	8.1	3.3	0.0	0.0	0.0	0.0	24.8	0.0	0.0	0.0	0.0	0.0	63.5
F	r_{max}	$\frac{B_{F_x}^2}{B_F^2}$ (%)							B_F	F	$\frac{B_F}{ F }$	D_F^\dagger	$\frac{B_F}{D_F}$		
		calib	acquis	u	v	r	\dot{u}	\dot{v}	\dot{r}	t	[N] [Nm]	[N] [Nm]	(%)	[N] [Nm]	(%)
	F_x	0.0	4.3	11.5	0.0	4.0	55.1	25.0	0.0	0.1	0.140	-10.06	1.4	-	-
F_y	0.150	0.0	2.1	7.1	0.0	89.8	0.0	1.0	0.0	0.606	-27.27	2.2	54.36	1.1	
M_z		0.4	2.0	0.8	0.0	95.8	0.1	0.9	0.0	0.0	0.457	-21.26	2.1	47.67	1.0
R	r_{max}	B_R	$\frac{B_R^2}{U_R^2}$	P_R	$\frac{P_R^2}{U_R^2}$	U_R	R	$\frac{U_R}{ R }$	D_R^\dagger	$\frac{U_R}{D_R}$					
		[10 ⁻²]	(%)	[10 ⁻²]	(%)	[10 ⁻²]	[-]	(%)	[-]	(%)					
	X'	0.081	24.7	0.142	75.3	0.163	-0.021	7.6	-	-					
Y'	0.150	0.167	94.2	0.042	5.8	0.172	-0.017	10.0	0.034	5.0					
N'		0.040	90.0	0.013	10.0	0.042	-0.015	2.8	0.031	1.4					

[†] D: Dynamic range of the variable $D = |max - min|$

Table 16 UA summary of pure yaw test ($r = r_{max}$).

Var. (x)	L_{pp}	T_m	x_G	y_G	m	I_z	ρ	u	v	r	\dot{u}	\dot{v}	\dot{r}	F	
R	Unit	m	m	m	kg	kgm ²	kg/m ³	m/s	m/s	rad/s	m/s ²	m/s ²	rad/s ²	N,Nm	
	Mag.	3.048	0.132	-0.016	0.000	82.55	49.79	998.1	1.518	0.269	0.000	0.000	0.001	-0.001	-
	B_x	0.002	0.001	0.005	0.002	0.11	1.84	0.041	0.010	0.008	0.000	0.000	0.000	0.000	-
X'	$\frac{\theta_x^2 B_x^2}{B_R^2}$	0.0	4.9	0.0	0.0	0.0	-	0.0	82.8	0.3	-	0.0	-	0.0	12.0
Y'	$\frac{B_R^2}{B_x^2}$	0.0	3.2	0.0	0.0	0.0	-	0.0	9.5	1.1	0.0	-	0.0	0.0	86.1
N'	(%)	0.1	3.5	0.0	0.0	0.0	0.0	0.0	10.5	0.2	0.0	0.0	0.0	0.5	85.2
F	v_{max}	$\frac{B_{F_x}^2}{B_F^2} (\%)$								B_F	F	$\frac{B_F}{ F }$	D_F^\dagger	$\frac{B_F}{D_F}$	
	[m/s]	calib	acquis	u	v	r	\dot{u}	\dot{v}	\dot{r}	t	[N] [Nm]	[N] [Nm]	(%)	[N] [Nm]	(%)
F_x		0.0	5.6	8.9	85.5	0.0	0.0	0.0	0.0	0.0	0.166	-13.91	1.2	-	-
F_y	0.269	0.0	0.7	0.0	99.2	0.0	0.0	0.1	0.0	0.0	1.168	-29.55	4.0	86.08	1.4
M_z		0.0	0.6	0.0	99.3	0.0	0.0	0.0	0.0	0.0	1.770	-47.10	3.8	94.46	1.9
R	v_{max}	B_R	$\frac{B_R^2}{U_R^2}$	P_R	$\frac{P_R^2}{U_R^2}$	U_R	R	$\frac{U_R}{ R }$	D_R^\dagger	$\frac{U_R}{D_R}$					
	[m/s]	[10 ⁻²]	(%)	[10 ⁻²]	(%)	[10 ⁻²]	[-]	(%)	[-]	(%)					
X'		0.100	35.4	0.135	64.6	0.168	-0.029	5.8	-	-					
Y'	0.269	0.264	91.2	0.082	8.8	0.276	-0.062	4.5	0.133	2.1					
N'		0.132	97.7	0.020	2.3	0.133	-0.032	4.1	0.065	2.1					


[†] D : Dynamic range of the variable $D = |max - min|$

Table 17 UA summary of pure sway test ($v = v_{max}$).

Var. (x)	L_{pp}	T_m	x_G	y_G	m	I_z	ρ	u	v	r	\dot{u}	\dot{v}	\dot{r}	F	
R	Unit	m	m	m	kg	kgm ²	kg/m ³	m/s	m/s	rad/s	m/s ²	m/s ²	rad/s ²	N,Nm	
	Mag.	3.048	0.132	-0.016	0.000	82.55	49.79	998.1	1.503	-0.263	0.151	0.001	0.004	0.000	-
	B_x	0.002	0.001	0.005	0.002	0.11	1.84	0.041	0.010	0.006	0.003	0.002	0.002	0.000	-
X'	$\frac{\theta_x^2 B_x^2}{B_R^2}$	0.0	3.8	0.0	0.0	0.0	-	0.0	60.2	1.5	2.2	8.8	-	0.0	23.5
Y'	$\frac{B_R^2}{B_x^2}$	0.0	2.8	0.0	0.0	0.1	-	0.0	2.6	0.5	16.1	-	2.0	0.0	76.0
N'	(%)	0.1	2.4	1.2	0.0	0.0	0.0	0.0	7.1	0.1	0.0	0.0	0.0	0.0	89.2
F	r_{max}	$\frac{B_{F_x}^2}{B_F^2} (\%)$								B_F	F	$\frac{B_F}{ F }$	D_F^\dagger	$\frac{B_F}{D_F}$	
	[rad/s]	calib	acquis	u	v	r	\dot{u}	\dot{v}	\dot{r}	t	[N] [Nm]	[N] [Nm]	(%)	[N] [Nm]	(%)
F_x		0.0	3.5	36.6	0.4	31.5	26.9	1.1	0.0	0.0	0.235	-15.78	1.5	-	-
F_y	0.151	0.0	0.0	13.3	36.7	45.8	0.3	3.9	0.0	0.0	0.872	2.94	29.7	67.48	1.3
M_z		0.1	0.4	1.8	53.0	38.5	0.2	5.9	0.1	0.0	0.896	19.54	4.6	66.37	1.4
R	r_{max}	B_R	$\frac{B_R^2}{U_R^2}$	P_R	$\frac{P_R^2}{U_R^2}$	U_R	R	$\frac{U_R}{ R }$	D_R^\dagger	$\frac{U_R}{D_R}$					
	[rad/s]	[10 ⁻²]	(%)	[10 ⁻²]	(%)	[10 ⁻²]	[-]	(%)	[-]	(%)					
X'		0.104	32.9	0.148	67.1	0.181	-0.027	6.8	-	-					
Y'	0.151	0.214	82.4	0.099	17.6	0.236	0.047	5.0	0.065	3.6					
N'		0.067	93.2	0.018	6.8	0.069	0.014	5.1	0.045	1.5					

[†] D : Dynamic range of the variable $D = |max - min|$

Table 18 UA summary of yaw and drift test ($r = r_{max}$).

	ITTC – Recommended Procedures and Guidelines	7.5-02 06-04 Page 21 of 25	
	Forces and moment Uncertainty Analysis, Example for Planar Motion Mechanism Test	Effective Date 2008	Revision 00

APPENDIX A Mean draft bias B_{T_m}

If the model ship is ballasted based on displacement, B_{T_m} is composed of two uncorrelated elemental errors, $B_{T_m,d1}$ from the model manufacturing error and $B_{T_m,d2}$ from the error related to ballast weights. By assuming the model error to be $\pm 1\text{mm}$ in all coordinates, as given in ITTC Procedure 7.5-01-01-01 Rev 01, 'Ship Models', and these dimensions are changed while keeping the block coefficient constant, the displacement of the model becomes

$$\nabla' = \rho(L + \varepsilon_L)(B + \varepsilon_B)(T + \varepsilon_T) \quad (\text{A1})$$

where, ρ is the water density, L , B , T are model length, beam, draft, respectively, and $\varepsilon_L=2\text{mm}$, $\varepsilon_B=2\text{mm}$, $\varepsilon_T=1\text{mm}$ are errors in length, beam, draft, respectively. Then $B_{T_m,d1}$ can be estimated as

$$B_{T_m,d1} = \frac{\nabla' - \nabla}{\rho A_{WP}} = 0.0011\text{m} \quad (\text{A2})$$

where A_{WP} is the water plane area of the model given in Table 1. $B_{T_m,d2}$ can be estimated from the total mass bias B_m by equating with the displacement change

$$B_{T_m,d2} = \frac{B_m}{\rho A_{WP}} = 0.0001\text{m} \quad (\text{A3})$$

Then, $B_{T_m} = 0.001\text{m}$ is estimated as the RSS of $B_{T_m,d1}$ and $B_{T_m,d2}$.

APPENDIX B.. Moment of inertia bias B_{I_z} .

Generally, yaw moment of inertia can be measured by measuring yawing periods T while swinging a given mass attached to, for example, a steel rod with known torsion stiffness G (*swinging method*), or by measuring the yaw moment while enforcing a sinusoidal yaw motion to the mass (*yawing method*).

If the *swinging method* is used, the moment of inertia of the mass is

$$I_z = GgT^2 \quad (\text{B1})$$

where g is the gravitational acceleration. The bias limit of the measured I_z can be estimated as:

$$B_{I_z}^2 = \theta_G^2 B_G^2 + \theta_T^2 B_T^2 \quad (\text{B2})$$

where, sensitivity coefficients are calculated by differentiating equation (B1) with respect to each variable. Elemental biases B_G and B_T should be estimated according to their test procedures used. Details of this method are provided in Simonsen C. (2004).

If the *yawing method* is used, the moment of inertia of the mass is determined from the motion equation of simple yaw:

$$-M_z = I_z \ddot{\psi}$$

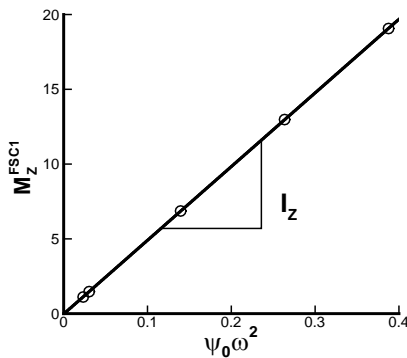
where, $\psi = -\psi_o \cos \omega t$ and M_z is the moment measured during the applied yaw motion. By expanding the measured moment with the FS series with the applied yaw motion frequency ω as the base frequency,

$$I_z = \frac{M_z^{FSC1}}{\psi_0 \omega^2} \quad (B3)$$

where, M_z^{FSC1} is the FS 1st harmonic amplitude of measured yaw moment, ψ_0 is the applied yaw motion amplitude, and $\omega = 2\pi N/60$ is the yaw motion frequency.

$$M_z^{FSC1} = \frac{2}{J} \sum_{j=1}^J M_{zj} \cos \omega t_j \quad (B4)$$

If multiple measurements with combinations of different ψ_0 's and ω 's are conducted, the yaw moment of inertia can be determined with a least-square (LS) regression method.



Hence the bias limit of the measured yaw moment of inertia B_{I_z} is considered as the RSS of each bias limit of individual measurement $B_{I_z,i}$ and error related to LS which is $B_{I_z,LS}$:

$$B_{I_z}^2 = \sum_i B_{I_z,i}^2 + B_{I_z,LS}^2 \quad (B5)$$

$B_{I_z,i}$ in equation (B5) can be defined as

$$B_{I_z,i}^2 = \theta_{M_z^{FSC1}}^2 B_{M_z^{FSC1}}^2 + \theta_{\psi_0}^2 B_{\psi_0,i}^2 + \theta_{\omega}^2 B_{\omega,i}^2 \dots \dots \dots (B6)$$

Sensitivity coefficients are calculated analytically from the equation (B5). $B_{M_z^{FSC1}}$ is defined from equation (B4),

$$B_{M_z^{FSC1}}^2 = \sum_{j=1}^J \theta_{M_z,i_j}^2 B_{M_z,i_j}^2 + \theta_{\omega_i}^2 B_{\omega_i}^2 + \sum_{j=1}^J \theta_{t_j}^2 B_{t_j}^2 \quad (B7)$$

where, $B_{\omega_i} = 2\pi B_N/60$. $B_{M_z,j}$ is estimated as 3% of $B_{M_z^{FSC1}}$. Finally $B_{I_z,LS}$ is quantified with the standard estimate of error (SEE) from Coleman and Steel (1999),

$$B_{I_z,LS} = \sqrt{\sum_{i=1}^L \frac{(I_z - I_{z,i})^2}{L-1}} \quad (B8)$$

where, I_z is the LS regression result and $I_{z,i}$ is the result of individual measurements.


If the yaw moment of inertia of the model ship is measured together with a mount or a yoke to hold the model ship, and if part of ballasting weights is added or removed while mounting, the yaw moment of inertia of the model is

$$I_z = I_{z,Total} - I_{z,mount} \pm \sum_k I_{z,ballast,k} \quad (B9)$$

where, I_z is the moment of inertia of the model, $I_{z,Total}$ is the total moment of inertia of combined model and mount or yoke, $I_{z,mount}$ is that of the mount or yoke, and $I_{z,ballast,k}$ is the moment of inertia of the ballast weights added or excluded. If the moment of inertia of each ballast weight with respect to its own axis and the distance to the mid ship are known, the moment of inertia of the ballast weight is calculated by using the parallel axis theorem

$$\sum_k I_{z,ballast,k} = \sum_k (I_{z,own,k} + r_k^2 m_k) \quad (B10)$$

where r_k is the distance to the mid ship and m_k

 INTERNATIONAL TOWING TANK CONFERENCE	ITTC – Recommended Procedures and Guidelines	7.5-02 06-04 Page 23 of 25	
	Forces and moment Uncertainty Analysis, Example for Planar Motion Mechanism Test	Effective Date 2008	Revision 00

is the weight of the ballast weight. By applying the error propagation equation to equation (B10), $B_{I_z,ballast,k}$ is

$$B_{I_z,ballast,k}^2 = \theta_{I_z,own,k}^2 B_{I_z,own,k}^2 + \theta_{r_k}^2 B_{r_k}^2 + \theta_{m_k}^2 B_{m_k}^2 \quad (B11)$$


Then B_{I_z} is

$$B_{I_z}^2 = B_{I_z,Total}^2 + B_{I_z,mount}^2 + \sum_k B_{I_z,ballast,k}^2 \quad (B12)$$

$B_{I_z,Total}$ and $B_{I_z,mount}$ can be estimated either from equation (B1) or (B5) according to I_z measurement method used, and $B_{I_z,ballast,k}$ can be estimated from equation (B10), respectively. An example with yawing method is presented in Table B.

	i	ψ_0	f	$M_{z,i}^{FSC1}$	$I_{z,i}$	$\theta_{M_{z,i}^{FSC1}}^2 B_{M_{z,i}^{FSC1}}^2$	$\theta_{\psi_0,i}^2 B_{\psi_0,i}^2$	$\theta_{\omega,i}^2 B_{\omega,i}^2$	$B_{I_z,i}$	$I_z - I_{z,i}$
		[deg]	[Hz]	[Nm]	[kgm ²]	[kgm ²]	[kgm ²]	[kgm ²]	[kgm ²]	[kgm ²]
Model	1	9.0	0.15	6.86	49.19	1.01E-03	1.45E+00	4.30E-05	1.20	5.16E-02
+	2	17.0	0.15	12.98	49.24	1.31E-02	4.06E-01	4.31E-05	0.65	2.69E-03
Mount	3	9.0	0.25	19.07	49.19	7.07E-02	1.45E+00	1.55E-05	1.23	5.05E-02
$B_{I_z}^2 = \sum_i^L B_{I_z,i}^2 + \left(2 \sqrt{\sum_i^L \frac{(I_z - I_{z,i})^2}{L-2}} \right)^2$; $I_{z,Total} = 49.19 \text{kgm}^2$, $B_{I_z,Total} = 1.84 \text{kgm}^2$										
Mount	1	9.0	0.15	0.15	1.05	7.67E-10	6.61E-04	1.97E-08	0.03	4.89E-02
	2	17.0	0.15	0.28	1.08	5.89E-09	1.95E-04	2.07E-08	0.01	2.23E-02
	3	9.0	0.25	0.42	1.08	1.92E-08	7.01E-04	7.51E-09	0.03	1.76E-02
$I_{z,mount} = 1.10 \text{kgm}^2$, $B_{I_z,mount} = 0.12 \text{kgm}^2$										
	k	Item	$I_{z,own,k}$	$\varepsilon_{I_{z,own,k}}$	m_k	ε_{m_k}	r_k	ε_{r_k}	$B_{I_{z,own,k}}$	
			[kgm ²]	[kgm ²]	[kg]	[kg]	[m]	[m]	[kgm ²]	
Ballast Weights	1	Part 1	0.0014	0.00006	1.109	0.02	0.0	0.001	0.00006	
	2	Part 2	0.0014	0.00006	1.109	0.02	0.75	0.001	0.01137	
	3	Part 3	0.0014	0.00006	1.109	0.02	0.75	0.001	0.01137	
	4	weight 1	0.0257	0.00047	2.285	0.04	0.118	0.001	0.00091	
	5	weights 6, 11, 12, 13	0.0726	0.00080	9.122	0.08	0.211	0.001	0.00531	
$I_{z,ballast} = \sum_k (I_{z,own,k} + r_k^2 m_k)$ $B_{I_{z,ballast}}^2 = \sum_k B_{I_{z,ballast,k}}^2$, $B_{I_{z,ballast,k}}^2 = \theta_{I_{z,own,k}}^2 B_{I_{z,own,k}}^2 + \theta_{r_k}^2 \varepsilon_{r_k}^2 + \theta_{m_k}^2 \varepsilon_{m_k}^2$ $I_{z,ballast} = 1.70 \text{kgm}^2$, $B_{I_{z,ballast}} = 0.017 \text{kgm}^2$										
$I_z = I_{z,Total} - I_{z,mount} + I_{z,ballast} = 49.79 \text{kgm}^2$ $B_{I_z} = \sqrt{B_{I_z}^2 + B_{I_{z,mount}}^2 + B_{I_{z,ballast}}^2} = 1.84 \text{kgm}^2$										

Table B. Moment of inertia bias limit B_{I_z} estimation.

	ITTC – Recommended Procedures and Guidelines	7.5-02 06-04 Page 24 of 25	
	Forces and moment Uncertainty Analysis, Example for Planar Motion Mechanism Test	Effective Date 2008	Revision 00

APPENDIX C

Carriage speed bias B_{U_C} .

Carriage speed bias limit B_{U_C} is estimated end-to-end by calibrating the carriage speed with respect to reference speeds. Reference speeds are obtained by measuring travel time Δt for a known distance ΔL .

$$U_{\text{ref}} = \frac{\Delta L}{\Delta t} \quad (\text{C1})$$

B_{U_C} is composed of two uncorrelated elemental errors; calibration error $B_{U_C, \text{calib}}$ and data-acquisition error $B_{U_C, \text{acquis}}$,

$$B_{U_C}^2 = B_{U_C, \text{calib}}^2 + B_{U_C, \text{acquis}}^2 \quad (\text{C2})$$

where, $B_{U_C, \text{calib}}$ is the RSS of the individual reference speed error,

$$B_{U_C, \text{calib}} = \sqrt{\sum_i (\theta_{\Delta L_i}^2 B_{\Delta L_i}^2 + \theta_{\Delta t_i}^2 B_{\Delta t_i}^2)} \quad (\text{C3})$$

where, $B_{\Delta L}$ and $B_{\Delta t}$ are the errors of ΔL and Δt , respectively. $B_{U_C, \text{acquis}}$ is quantified with the standard estimate of error (SEE) as per ITTC guidelines

$$B_{U_C, \text{acquis}} = 2SEE = 2\sqrt{\frac{\sum_i (U_{C,i} - U_{\text{ref},i})^2}{N-2}} \quad (\text{C4})$$

Carriage speed measurement results are summarized in Table C.

APPENDIX D

Drift angle bias B_β .

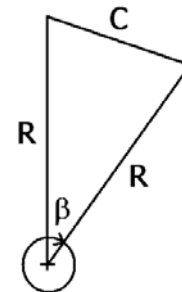
Drift angle bias limit B_β is composed of two uncorrelated elemental errors $B_{\beta, \text{align}}$ and $B_{\beta, \text{drift}}$.

$$B_\beta = \sqrt{B_{\beta, \text{align}}^2 + B_{\beta, \text{drift}}^2} \quad (\text{D1})$$

$B_{\beta, \text{align}}$ is the model ship installation error with respect to straight towing direction and assumed to be 0.03° . $B_{\beta, \text{drift}}$ is the deviation from designated drift angle setting and it is estimated end-to-end by calibrating the drift angle with respect to reference angles. Reference angle is achieved by measuring the chord length of the arc swept by a fixed position on the model ship due to drift angle setting.

$$\beta_{\text{ref}} = \cos^{-1}\left(1 - \frac{C^2}{2R^2}\right) \quad (\text{D2})$$

The concept of reference angle measurement is illustrated as



where, C is the chord length measured, R is the distance between mid ship and the measurement position. Then $B_{\beta, \text{drift}}$ can be further decomposed into two uncorrelated elemental er-

rors $B_{\beta,calib}$ and $B_{\beta,acquis}$. The procedure to estimate these errors is similar with B_{U_c} estimation. $B_{\beta,drift}$ measurement results are summarized in Table D. Finally, $B_{\beta}=0.222^\circ$ is estimated from the RSS of $B_{\beta,align}$ and $B_{\beta,drift}$.

i	ΔL_i [m]	Δt_i [s]	$U_{ref,i}$ [m/s]	$U_{C,i}$ [m/s]	$B_{U_c,calib,i}$ [m/s]
1	24.088	30.6301	0.7864	0.7840	0.000163
2	24.088	30.6985	0.7847	0.7823	0.000163
3	24.088	30.7130	0.7843	0.7816	0.000163
4	14.989	11.5026	1.5639	1.5601	0.000435
5	14.989	11.5102	1.5629	1.5590	0.000435
6	14.989	11.5204	1.5615	1.5576	0.000434
7	14.989	4.9269	2.2694	2.2631	0.000631
8	14.989	4.9315	2.2681	2.2619	0.000631
9	14.989	4.9273	2.2693	2.2629	0.000631

$$B_{\Delta L}=0.005m, B_{\Delta t}=0.0001sec$$

$$B_{U_c,calib} = \sqrt{\sum_i (\theta_{\Delta L_i}^2 B_{\Delta L_i}^2 + \theta_{\Delta t_i}^2 B_{\Delta t_i}^2)} = 0.0014m/s$$

$$B_{U_c,acquis} = 2\sqrt{\sum_i \frac{(U_{C,i}-U_{ref,i})^2}{N-2}} = 0.0102m/s$$

$$B_{U_c} = \sqrt{B_{U_c,calib}^2 + B_{U_c,acquis}^2} = 0.0102m/s$$

Table C. Carriage speed bias limit B_{U_c} .

i	R_i [m]	C_i [m]	$\beta_{ref,i}$ [deg]	β_i [deg]	$B_{\beta,calib,i}$ [deg]
1	1.998	0.068	1.96	2.00	0.00050
2	1.998	0.137	3.94	4.00	0.00050
3	1.998	0.207	5.94	6.00	0.00050
4	1.998	0.276	4.93	8.00	0.00050
5	1.998	0.344	9.87	10.00	0.00050
6	1.998	0.414	11.88	12.00	0.00051
7	1.998	-0.067	-1.93	-2.00	0.00050
8	1.998	-0.137	-3.92	-4.00	0.00050
9	1.998	-0.206	-5.92	-6.00	0.00050
10	1.998	-0.275	-4.88	-8.00	0.00050
11	1.998	-0.343	-9.84	-10.00	0.00050
12	1.998	-0.413	-11.86	-12.00	0.00051

$$\beta_{ref,i} = \cos^{-1}\left(1 - \frac{C_i^2}{2R_i^2}\right); \quad \varepsilon_R = \varepsilon_C = 0.001m$$

$$B_{\beta,calib,i} = \sqrt{\theta_{R_i}^2 \varepsilon_R^2 + \theta_{C_i}^2 \varepsilon_C^2}$$

$$B_{\beta,calib} = \sqrt{\sum_i B_{\beta,calib,i}^2} = 0.002^\circ$$

$$B_{\beta,acquis} = 2\sqrt{\sum_i \frac{(\beta_i - \beta_{ref,i})^2}{N-2}} = 0.222^\circ$$

$$B_{\beta,drift} = \sqrt{B_{\beta,calib}^2 + B_{\beta,acquis}^2} = 0.222^\circ$$

Table D. Drift angle bias limit B_{β} .